

393452  
P

**NASA contract S85188Z: Final Report**

**Study of the Zodiacal Cloud (Dust Bands) in the near-IR.**

**By**

**Dr. Sumita Jayaraman**

**submitted to**

**NASA Astrophysics Data Program**

## Introduction

The zodiacal cloud is populated by cometary, asteroidal (Leinert and Grün, 1985) and recently, interstellar, dust particles (Grün et al., 1994) each with its own distinct particle properties and spatial distribution. One of the main limitations in understanding the structure and the origin of the cloud is that all observations yield the integrated flux along any given line of sight, making it difficult to identify both the type of source and the location of the radiation. This problem can be overcome by studying individual structures in the cloud that are associated with a specific source, for example, using the zodiacal dust bands that have an asteroidal origin can help us to model the asteroidal component of the cloud.

This report presents the latest results from the ongoing project to study and understand the fine structure of the zodiacal cloud. In this project we have concentrated upon the near-infrared (near-IR) observations of the zodiacal cloud by the Diffuse Background Infrared Experiment (DIRBE) aboard the Cosmic Background Explorer satellite (COBE). At thermal wavelengths ( $> 4\mu\text{m}$ ) the radiation from the zodiacal cloud is the dominant source of the background flux brought about by the heat radiated from the solar system dust particles. However, in the near-IR wavebands the signal is generated by scattered sun light and the flux decreases by more than an order of magnitude from the thermal emission. Therefore, it is a challenge to study the structures, easily detected in thermal emission, in the near-IR.

### DIRBE-COBE Data Set in the near-IR bands:

The DIRBE instrument aboard the COBE satellite was a ten band photometer measuring absolute fluxes by chopping between the sky and an internal reference source. The short term and long term photometric stability has been reported to be better than 1% (Spiesman et al., 1995). The detectors have a  $0.7^\circ$  by  $0.7^\circ$  field of view, and the satellite covered solar elongation angles between  $64^\circ$  and  $124^\circ$ . The instrument was in operation for 10 months from December 1990 and the initial data products were released in 1994 (COBE Explanatory Supplement). When the cryogen ran out, data collection from six of the 10 bands was discontinued. Fortunately, the instrument continued to map the sky in the four near infrared spectral wavebands at 1.25, 2.2, 3.5 and 4.9 microns. At the end of 1993 when the mission drew to a close, the instrument had acquired a vast quantity of data covering three years. These data have a lower signal to noise ratio because a) the contribution of stellar point sources emission that negligible at longer wavelengths but cannot be overlooked in the spectral bands, b) the decrease in the zodiacal brightness by at least an order of magnitude and c) the increase in the ambient temperature after the depletion of the cryogen. However, this is a unique data set consisting of a redundantly sampled map of the zodiacal sky because DIRBE covers nearly half the sky in one day. The same source, Sirius, was used for absolute calibration for all the bands which can give a higher accuracy in color determination. The data set used is the weekly averaged data that has 41 weeks of redundant coverage of the sky.

The first step in the analysis of the zodiacal cloud is to simulate scans in ecliptic latitude at constant solar elongation angle. As the line-of-sight of the telescope passes closer to the sun with decreasing solar elongation angle, the overall flux of the background increases as we sample hotter particles along the line of sight. Therefore, a set of scans each at a constant solar elongation angle samples particles at different radial distance from the sun at least near the

ecliptic plane. Figure. 1 shows a sample scan created at  $1.2\mu\text{m}$ . Although the zodiacal cloud is much weaker the underlying shape is evident. In addition there are numerous point sources at all latitudes and the galactic plane is the broad peak below the ecliptic.

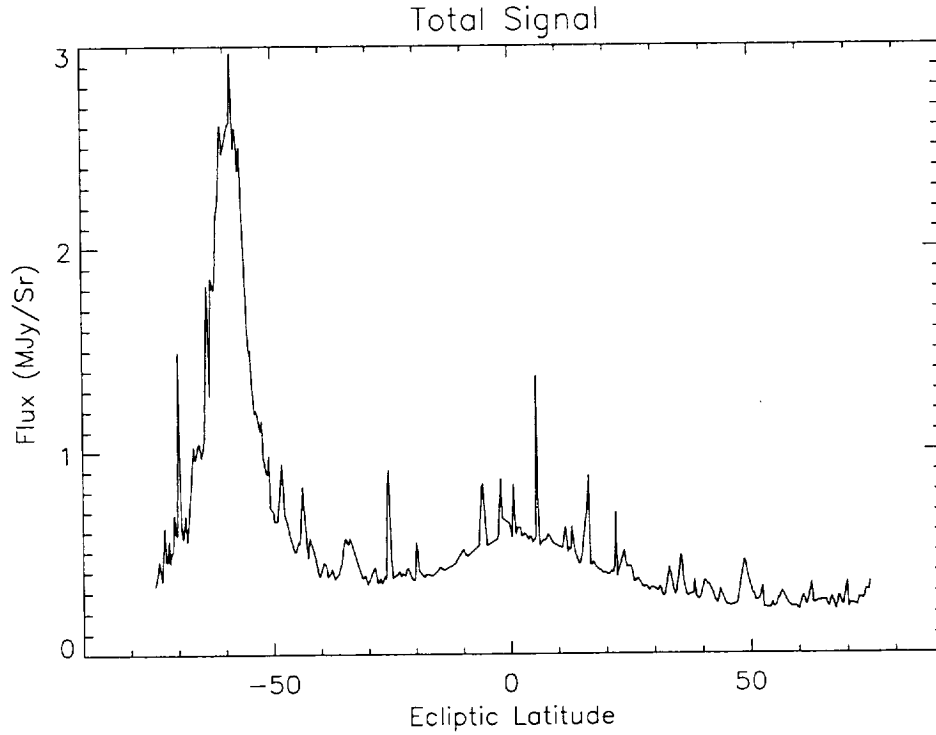


**Figure 1:** A sample scan at a constant solar elongation of  $75^\circ$  in band 1 (1.2 microns).

The second step in the analysis is to separate the smooth low frequency component of the zodiacal cloud from the high frequency fine structure. We use a fourier filter technique which separates out the low frequency background using a coefficient between 0 and 1 that determines the number of frequency components that are included. The filter also incorporates a 'parzen' windowing method that decreases frequency leakage. Before the filter is applied to the scan, the signal is pre-processed to remove the very bright point sources from the image. This is important for studying the high frequency component. Figure 2 and 3 show both components obtained after applying the median filter and the parzen Fourier filter to the scan in Figure 1.

Initially we had hoped to apply SKY model by Cohen to estimate the sky contribution to the stellar sources but the model is applicable only in band 3 (at 3.4 microns) and is a very strong function of the magnitude limit chosen for the stars.

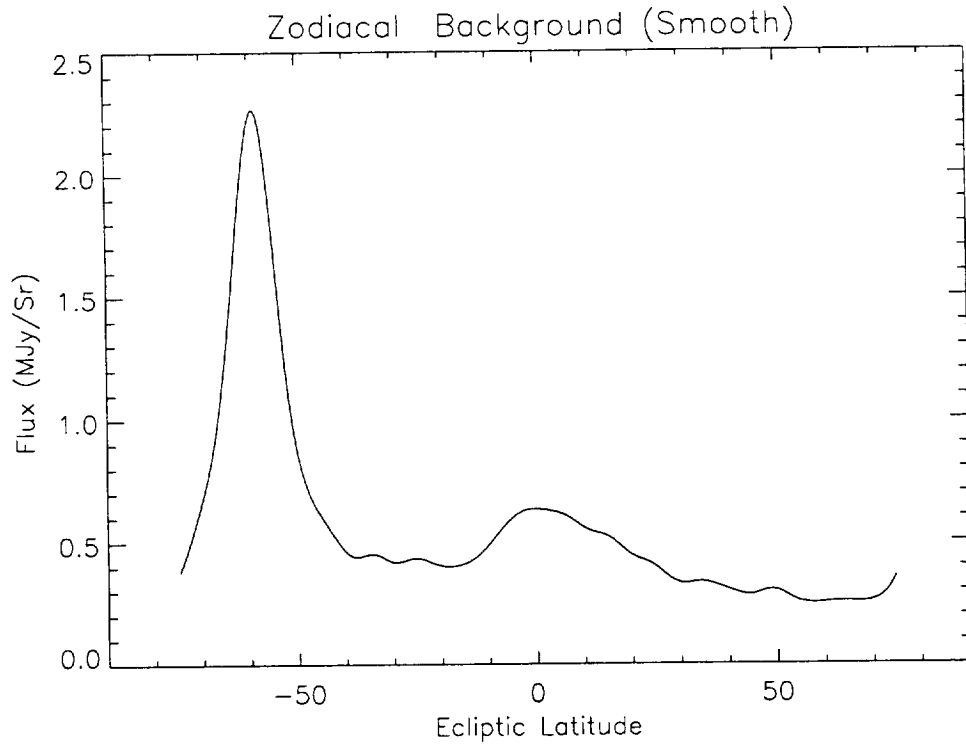


**Figure 2:** The low frequency component shows the smooth zodiacal background and the galactic plane after applying a fourier filter to the scan in Figure 1.

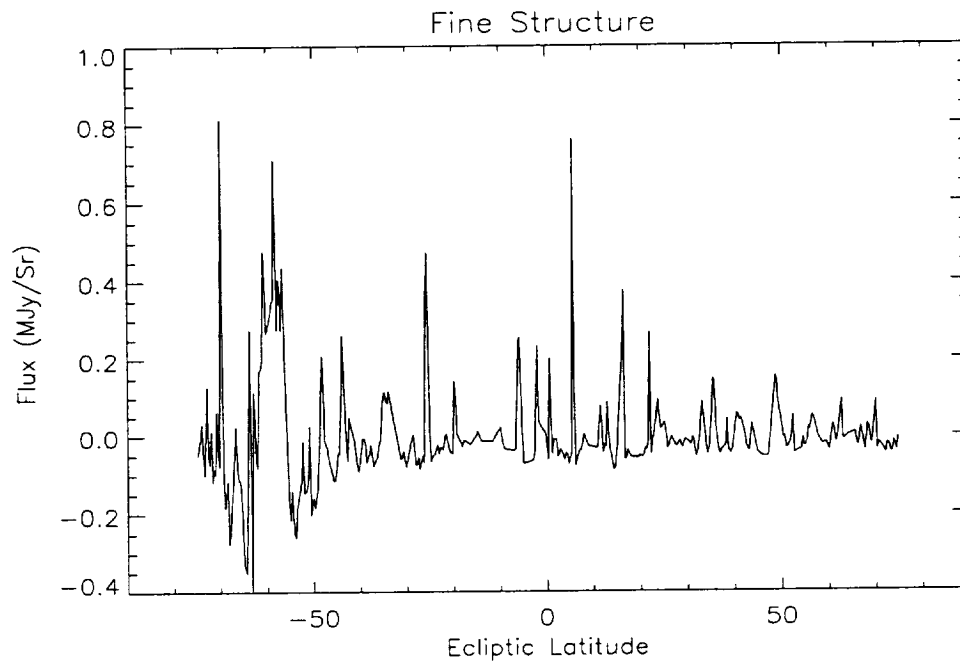


**Figure 3:** The high frequency component after applying a fourier filter to the scan in Figure 1 which has the fine structure of the zodiacal cloud but is extremely noisy due to a high number of point sources.

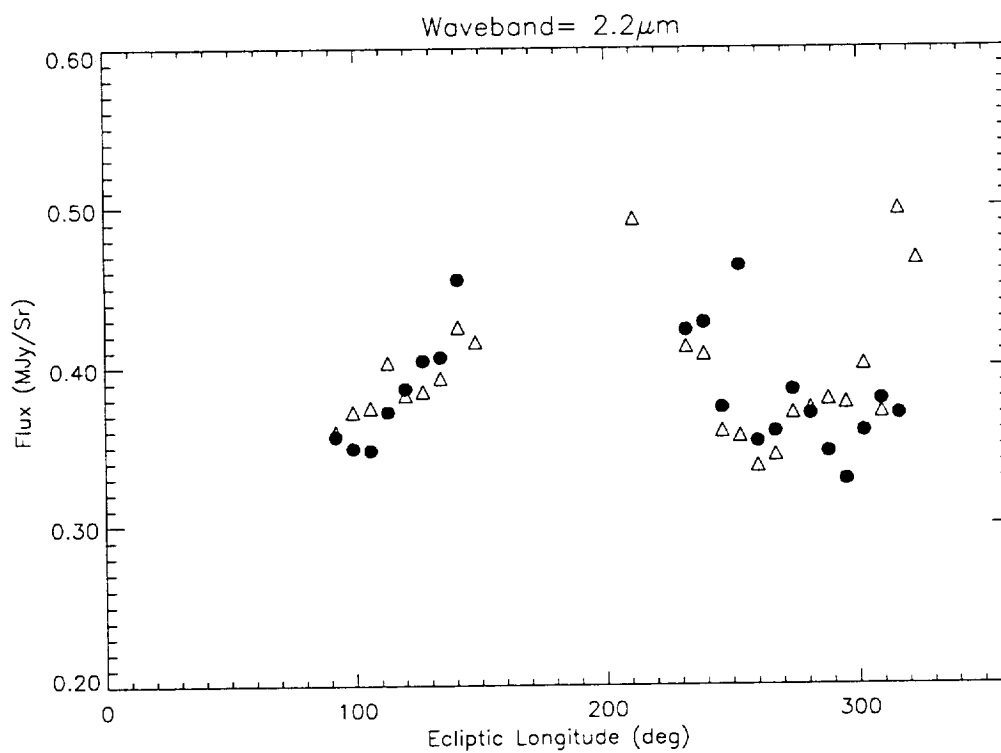
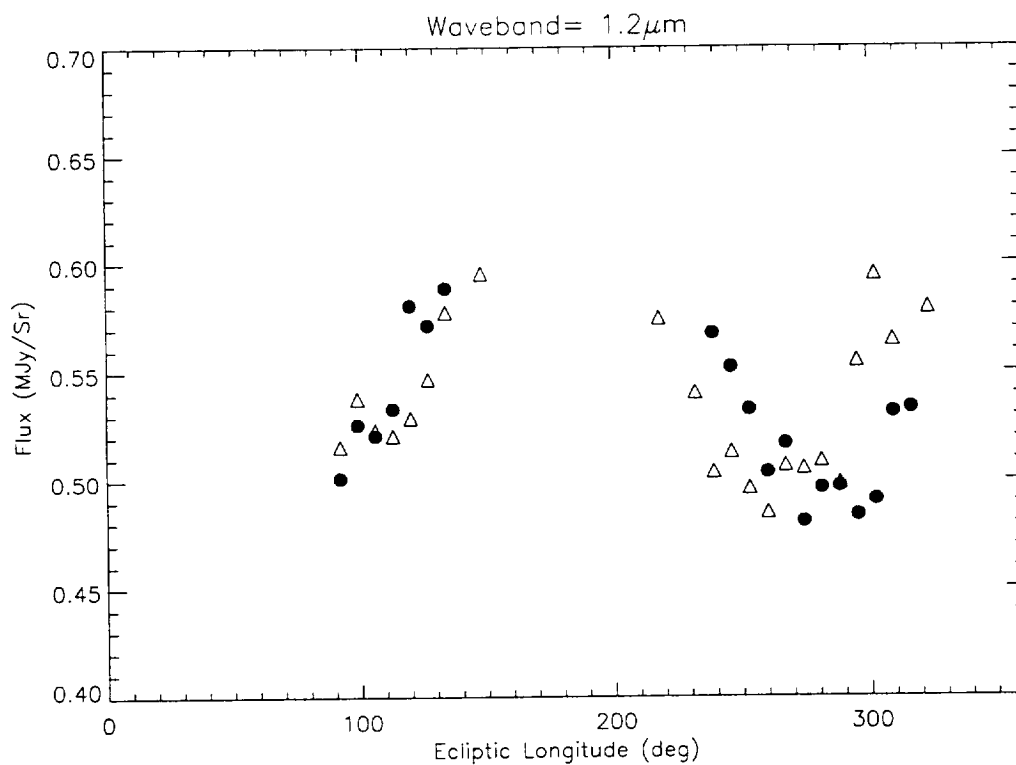
## Systematic Variations of the Zodiacal Light:

We first present the results of the study of the smooth background flux in scattered light. The data analysis was done in the following steps.

- a) Each week of data was first divided into two sets identified as Leading and Trailing data. As the COBE satellite was in a polar orbit, half the observations were taken in the descending orbit (Leading) while the other half in the ascending (Trailing) orbit. It is important to distinguish the two observations due to the presence of the asymmetry caused by the Earth's ring.
- b) The scans were simulated at elongation angles between  $65^\circ$  and  $124^\circ$  at every  $1^\circ$  for each week of data.
- c) The 'parzen' filter (described in the previous section) was applied to all the scans and peak of the smooth background was calculated for each week of data. The weeks for which the Galactic plane fell very near the ecliptic were not used.
- d) For each week, the peak flux (near the ecliptic) was plotted as a function of the solar elongation and the a normalized value of the peak flux at a constant solar elongation of  $90^\circ$  was calculated, again using a simple first of second order polynomial fit. A value of  $90^\circ$  is chosen as it has some special symmetry characteristics. The value of ecliptic longitude also remains along the scan at this elongation. In addition the line-of-sight  $180^\circ$  away in ecliptic longitude is also at  $90^\circ$  solar elongation.
- e) The annual systematic variation of the zodiacal background is measured by plotting the peak flux as a function of time.

Figure 3, 4 and 5 show the results of the extensive data reduction by the variation of the peak zodiacal flux in the three near-IR wavebands as function of ecliptic longitude of the Earth which corresponds to time of year. The filled circles denote data taken in the leading direction (in the direction of the Earth's motion along its orbit) while the open triangles represent trailing data. We see that there is a systematic variation of the flux which is due to the Earth moving through a rotationally asymmetric zodiacal cloud in an elliptical orbit. The flux is a minimum close to the perihelion of the Earth at  $104^\circ$ .

The other important effect that was being sought was the increased flux in the trailing direction at all times of the year. This is caused by a cloud of dust particles that follow the Earth in its orbit. The dust particles are a part of the Earth's circumsolar ring formed by resonant trapping of the low eccentricity asteroidal dust particles as they drift towards the sun from the Asteroid Belt due to P-R drag. We see that at 1.2 and 2.2 microns there is no evidence of the ring while there is a slight indication of the asymmetry which is not quantifiable within the errors.



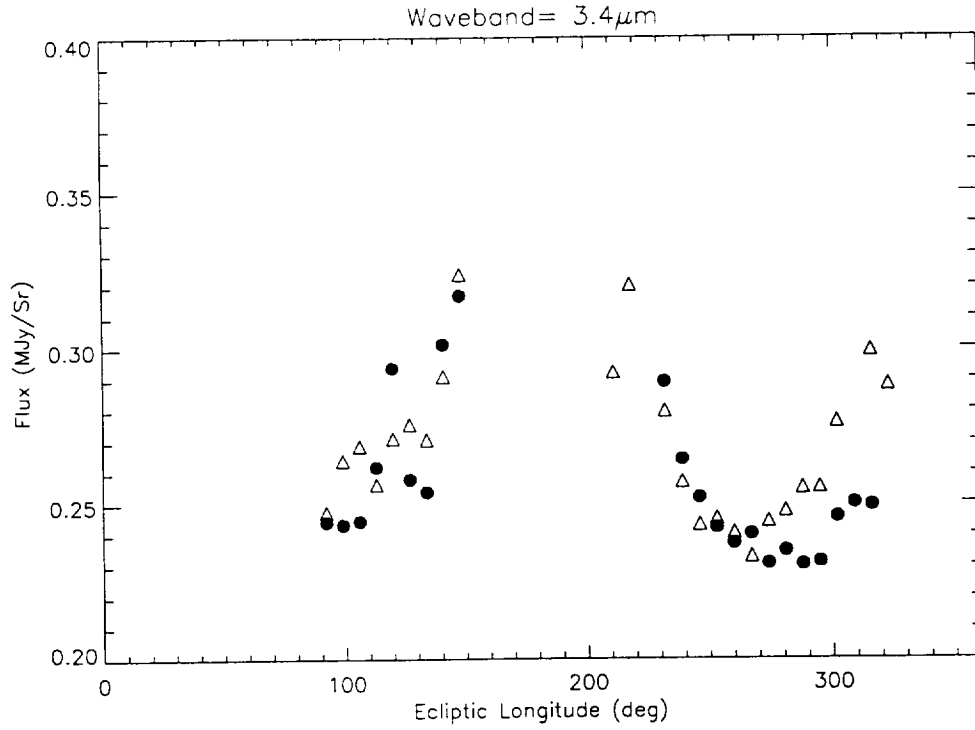


**Figure 3,4, 5:** The annual variation of the zodiacal peak flux in three DIBE near-IR bands.

### Zodiacal Dust Bands:

The zodiacal dust bands are high frequency structures clearly visible as symmetrically placed ‘bumps’ above the smooth zodiacal background and it is conventional to study them separately. The dust bands are formed by the collisional evolution of asteroids in Hirayama families (Dermott et al., 1984). Asteroids within a family have similar semi-major axes, eccentricities and inclinations because they are formed by the breakup of a single parent asteroid.

Although the asteroids themselves are located in the main belt, the dust produced from their collisional evolution extends all the way to the sun due to solar radiation pressure forces in time scales similar to their orbital precession. This leads to the formation of a three dimensional torus, the edges of which have a higher density of orbits and rise above the background zodiacal cloud to form two bands, above and below the ecliptic, for each family. Thus, the visible part of the dust bands is only 10% of the total contribution from the families (Dermott et al., 1994) as most of the dust is indistinguishable from the background. The dust bands are extremely important features because we can identify them with a specific family, which helps us to isolate and study the not only the asteroidal component of the zodiacal cloud but also identify characteristics of dust particles belonging to individual families.

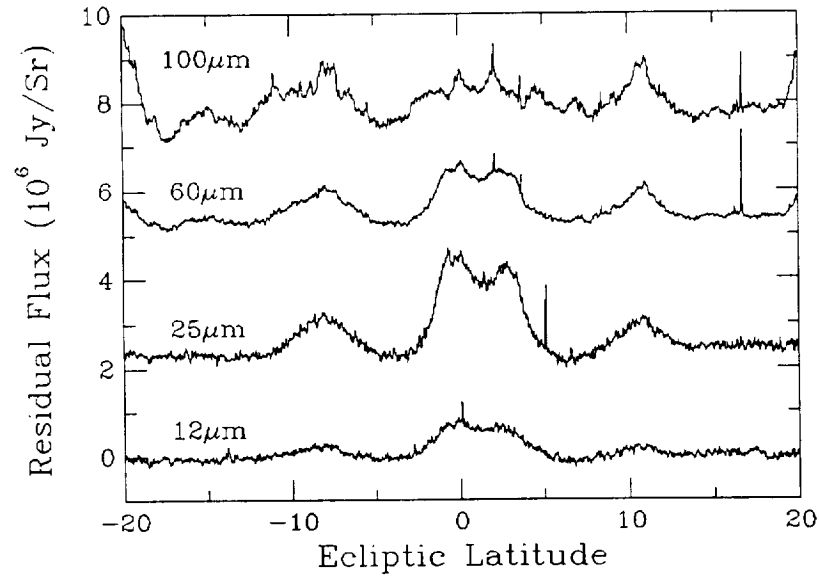


**Figure 6:** The dust bands in four infrared wavebands of IRAS with resolution of 2 arcminutes. The zodiacal cloud has been filtered out using a fast Fourier filter.

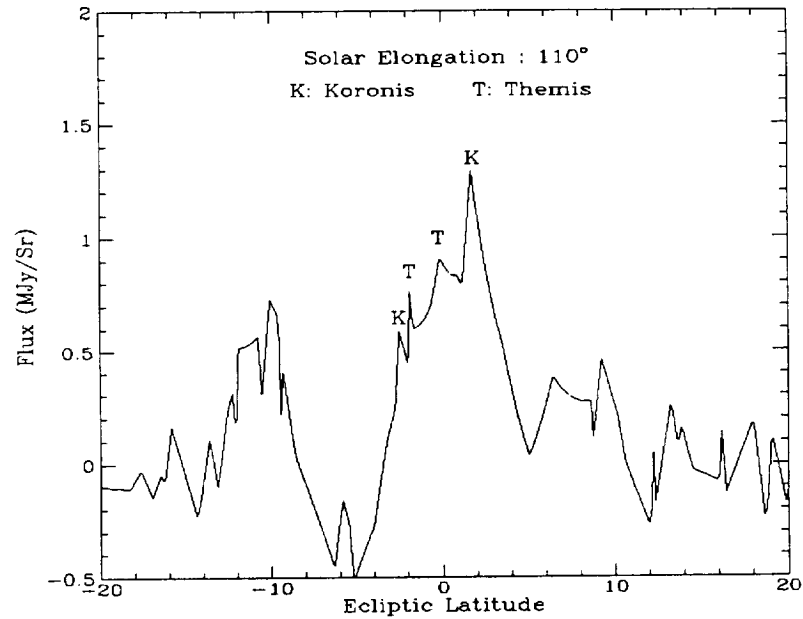


**Figure 7:** A scan from the DIRBE data in the 25 micron waveband after filtering the smooth zodiacal cloud shows evidence of the two pairs of dust bands present in the near-ecliptic band pair.

There are two prominent band pairs, one at  $\pm 10^\circ$  and the other near the ecliptic (Figure 6). The method of co-adding is so effective that the near-ecliptic bands have been further resolved into two bands at 0.01% of the total background signal. The two ecliptic band pairs are associated with two distinct families, Koronis and Themis (Sykes, 1992), while the ten-degree band is presumed to be associated with Eos although conclusive evidence has yet to be found.



(Dermott et al., 1992). Co-adding also becomes invaluable for extracting dust bands from the 100 micron waveband where the signal from the Galaxy interferes strongly with the solar system emission and it is impossible to detect the dust bands in an individual profile or even after co-adding over a few weeks of data. A sample of the low resolution COBE dust bands is shown in Figure 7 with the location of the primary asteroid families near the Ecliptic.

### Dust Bands in Scattered Light:

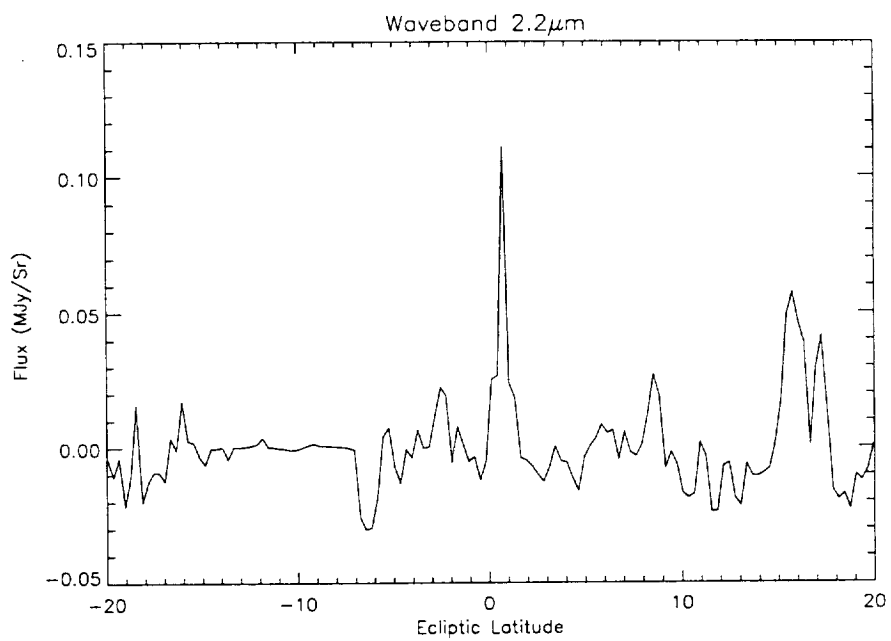
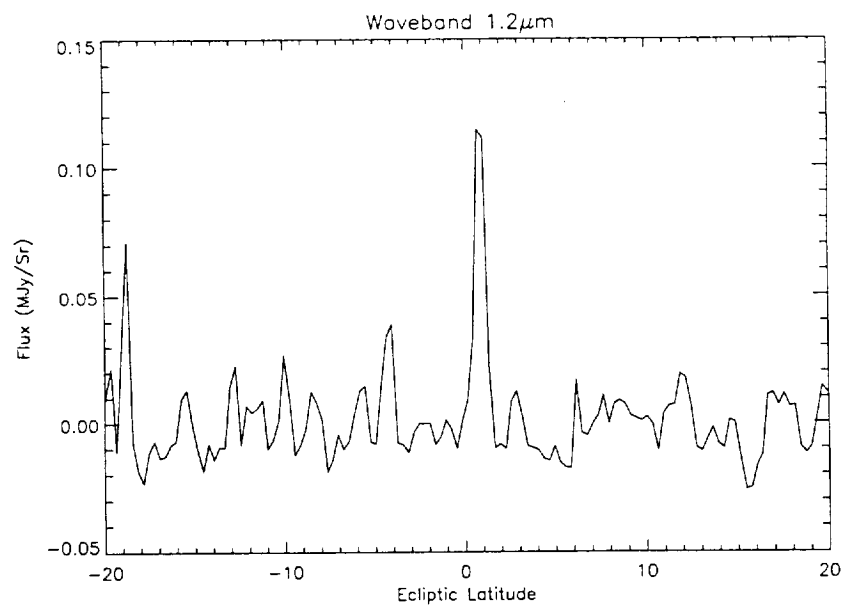
The zodiacal dust bands in scattered light have been detected by Spiesman (1995). However, they are very difficult to detect in the infrared because of the faint structure and the profusion of point sources. The data set used here is the high frequency component of the filtered signal shown in Figure 3.

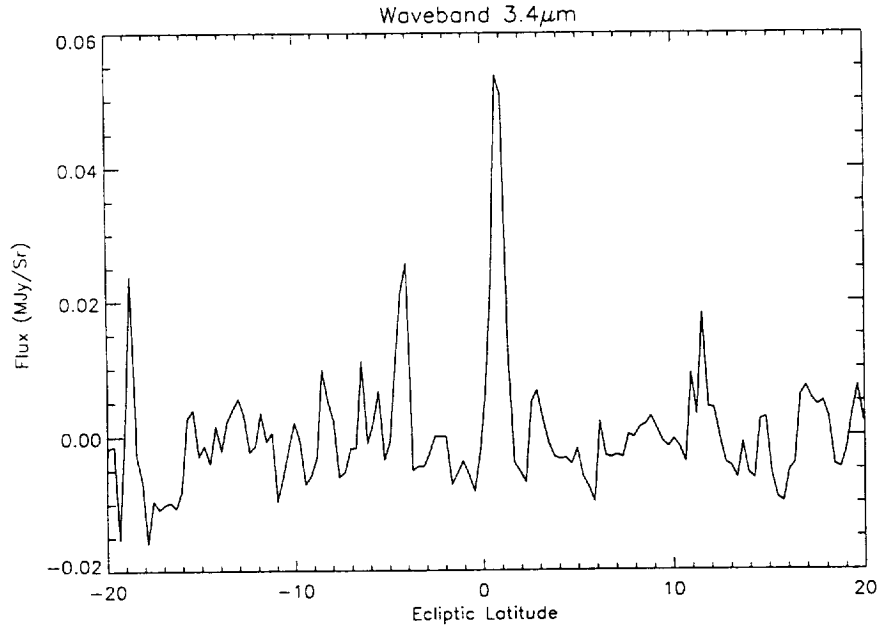
Here we use a method similar to that outline in the section for the smooth zodiacal background in order to co-add as many scans as possible to bring out the primary dustbands. The first three steps are the same as that for the smooth background. After obtaining the filtered scan, we use the scan for band 5 (12 microns) to fit polynomials to the ten-degree dustband pair. There are two different effect that have to be accounted for before co-addition.

- a) The distance between the pair (one above and the other below the ecliptic), denoted as  $\beta$ , is plotted as a function of solar elongation. Increasing solar elongation results in lines-of-sight away from the sun towards the Asteroid Belt while smaller solar elongations look towards the sun. This introduces a parallax effect in the dust band pair such that the distance between the north and south bands increase with solar elongation. Therefore, the slope of the curve that defines the  $\beta$  with elongation is a measure of the parallax effect. This slope is now used to correct individual scans by using  $\beta$  at solar elongation of  $90^\circ$  as the normalizing value and is applied as 'stretch' or 'shrink' parameter for elongations less than and greater than  $90^\circ$ , respectively.
- b) The second correction is brought about by the fact that the dust bands are not parallel to the ecliptic. The inclination of plane of symmetry of the dust bands is brought about by long term planetary perturbations on the dust particles. The annual variation in the location of the dust bands is used to determine the inclination. Once the inclination is found, the correction is a 'shift' given by  $A \sin(\lambda + \phi)$  where  $A$  is the amplitude,  $\lambda$  is the ecliptic longitude of the Earth and  $\phi$  is the phase. The values at 12 microns have been obtained previously (Dermott 1992) and are as follows:

Trailing:  $A = 1.25^\circ$  ;  $\phi = 203.81^\circ$

Leading:  $A = 1.14^\circ$  ;  $\phi = 347.42^\circ$





**Figures 8,9 and10:** The dust bands obtained from coadding the high frequency components at all elongations at three of the DIRBE near-IR bands.

The results of the coaddition are shown in Figures 8, 9 and 10. It is very easy to detect the near-ecliptic dustband at all three wavebands while the ten-degree bands are visible only above or below the ecliptic at 1.2 and 2.2 microns. The zodiacal flux is a minimum near 3.4 microns hence it is far more difficult to detect them in band 3. The flux in the central dustbands are 0.113, 0.115 and 0.054 MJy/Sr in bands 1, 2 and 3 respectively.

The data analyses presented in this report is part of an ongoing project to map the zodiacal cloud at all elongations and wavebands. The results will be published in *Icarus* in the near future.

Work is currently being pursued to study the data set released by NASA after subtracting a zodiacal cloud model. The effectiveness of the model will be measured by comparing the results to that of the filtering process. In addition, results from the Midrange Space Explorer (MSX) at much smaller elongations (25-30°) are also being studied to sample the dust particles distribution very close to the sun.

#### **4. References**

- Cohen, M., 1994. *Astron. J.*, 107, 582.
- Dermott, S.F., Nicholson, P.D., Burns, J.A. and Houck, J.R., 1985. In 'Properties and Interactions of Interplanetary Dust', (Eds. R.H. Giese and P. Lamy), D. Reidel Publishing Company, p 395-409.
- Dermott, S.F., Nicholson, P.D. and Wolven, B. 1986. In *Asteroids, Comets and Meteoros II* (eds. C.-I. Lagerkvist, B.A.Lindblad, H. Lundstedt and H. Rickman), Reprocentralen HSC, Uppsala, pp 583-594.
- Dermott, S.F. and Nicholson, P.D. 1989. *Highlights of Astronomy*, 8, 259-266.
- Dermott, S.F., Gomes, R.S., Durda, D.D., Gustafson, B.A.S., Jayaraman, S., Xu, Y.L. and Nicholson, P.D., 1992. In 'Chaos, Resonances and Collective Dynamical Phenomena in the Solar System', (Ed. S. Ferraz-Mello), Kluwer, Dordrecht, p 333-347.

- Dermott, S.F., Durda, D.D, Gustafson, B.A.S., Jayaraman, S., Liou, J.C., and Xu, Y.L., 1994. In *Asteroids Comets and Meteors*, 1993 (Eds. A. Milani, M. Martini and A. Cellino), Kluwer, Dordrecht, p 127-142.
- Dermott, S.F., Jayaraman, S., Xu, Y.L., Gustafson, B.A.S., and Liou, J.C., 1994. *Nature*, 369, 719-723.
- Dermott, S.F., Grogan, K., Gustafson, B.A.S., Jayaraman, S., Kortenkamp, S., and Xu., Y.L. 1996. In 'Physics, Chemistry and Dynamics of Interplanetary Dust' (In press)
- Grün, E., Gustafson, B.A.S., Mann, I., Baghul, M., Morfill, G.E., Staubach, P., Taylor, A. and Zook, H.A., 1994. *Astron. & Astrophys.* 286, 915.
- Gustafson, B.A.S., 1994. *Ann. Rev. Earth Planet. Sci.*, 22, 553-595.
- Jayaraman, S. and Dermott, S.F., 1995. In 'Unveiling the Comic Infrared Background'. (In press)
- Jayaraman, S. and Dermott, S.F. 1996. *Icarus* (submitted)
- Leinert, C. and Grün, E., 1985. In *Physics of the Inner Heliosphere* , (eds. R. Schwenn and E. Marsch,), Springer -Verlag, pp 207-275.
- Low, F.J., Neitema, D.A., Gautier, T.N., Gillett, F.C., Beichman, C.A., Neugebauer, G., Young, E., Aumann, H.H., Bogess, N., Emerson, J.P., Habing, H.J., Hauser, M.G., Houck, J.R., Rowan-Robinson, M. Soifer, B.T., Walker, R.G. and Wesselius, P.R., 1984. *Astrophys. J.*, 278:L19-L22.
- Reach, W.T., 1991. *Icarus*, 369, 529-543.
- Reach, W.T., 1992. *Icarus*, 392, 289-299.
- Reach, W.T., Franz, B.A., Weiland, J.L., Hauser, M.G., Kelsall, T., Wright., E.L., Tawley, G., Stemwedel, S.W., and Spiesman, W.,J., 1995. *Nature*, 374, 521-523.
- Spiesman, W.J, Hauser, M.G., Kelsall, T., Lisse, C..M., Moseley, S.H., Reach, W.T., Silverberg, R.F., Stemwedel, S. W., and Weiland, J.L., 1995. *Astrophys. J.*, 442, 662-667.
- Sykes, M.V., Greenberg, R.J., Dermott, S.F., Nicholson, P.D., Burns, J.A., and Gautier, T.N., 1989. In 'Asteroids II' (Eds. R. Binzel, T. Gehrels and M. Matthews), Univ. of Arizona Press, p 336-367.
- Sykes, M.V., 1992. *Icarus*, 95, 244-254.

REPORT DOCUMENTATION PAGE			Form Approved OMB No. 0704-0188	
Public reporting burden for this collection of information is estimated to average 1 hour per response, including the time for reviewing instructions, searching existing data sources, gathering and maintaining the data needed, and completing and reviewing the collection of information. Send comments regarding this burden estimate or any other aspect of this collection of information, including suggestions for reducing this burden, to Washington Headquarters Services, Directorate for Information Operations and Reports, 1215 Jefferson Davis Highway, Suite 1204, Arlington, VA 22202-4302, and to the Office of Management and Budget, Paperwork Reduction Project (0704-0188), Washington, DC 20503.				
1. AGENCY USE ONLY (Leave blank)		2. REPORT DATE April 1999		3. REPORT TYPE AND DATES COVERED Contractor Report
4. TITLE AND SUBTITLE Studying the Fine Structure and Temporal Variations of the Zodiacal Cloud and Asteroidal Dust Bands Using the 3-Year Near-IR COBE-DIRBE Data (Final Report)			5. FUNDING NUMBERS  S-85188-Z	
6. AUTHOR(S)  PI: Sumita Jayaraman				
7. PERFORMING ORGANIZATION NAME(S) AND ADDRESS (ES)  Vanguard Research, Inc. 10400 Eaton Place, Suite 450 Fairfax, VA 22030			8. PERFORMING ORGANIZATION REPORT NUMBER	
9. SPONSORING / MONITORING AGENCY NAME(S) AND ADDRESS (ES)  National Aeronautics and Space Administration Washington, DC 20546-0001			10. SPONSORING / MONITORING AGENCY REPORT NUMBER  NASA/CR-1999-209246	
11. SUPPLEMENTARY NOTES				
12a. DISTRIBUTION / AVAILABILITY STATEMENT  Unclassified-Unlimited Subject Category: 90 Report available from the NASA Center for AeroSpace Information, 7121 Standard Drive, Hanover, MD 21076-1320. (301) 621-0390.			12b. DISTRIBUTION CODE	
13. ABSTRACT (Maximum 200 words)  The report presents the results of the data analyses of the DIRBE-COBE data set to study the structure of the zodiacal cloud in the near-infrared wavebands at 1.2, 2.2, and 3.4 microns. The cloud has been divided into two components which have been analyzed and studied separately. The annual variation of the flux in the smooth or low frequency component has been measured in all three bands and the presence of any asymmetries due to the Earth's resonant ring have been studied.  The high frequency component which primarily consisted of the asteroidal dust bands. Extensive and careful coaddition was done to extract the central bands in all three wavebands. The ten-degree bands are present in the 1.2 and 2.2 microns but not in the 3.4 micron waveband.				
14. SUBJECT TERMS COBE/DIRBE, Asteroidal Dust Bands, Near-IR			15. NUMBER OF PAGES 11	
			16. PRICE CODE	
17. SECURITY CLASSIFICATION OF REPORT Unclassified	18. SECURITY CLASSIFICATION OF THIS PAGE Unclassified	19. SECURITY CLASSIFICATION OF ABSTRACT Unclassified	20. LIMITATION OF ABSTRACT UL	